

Bit error rate analysis of the spatial X-ray communication system

Li Yao^{1,2}, Su Tong^{*1,2}, Shi Feng³, Sheng Lizhi¹, Qiang Pengfei^{1,2}, Zhao Baosheng¹

(1. State Key Laboratory of Transient Optics and Photonics, Xi'an Institute of Optics and Precision Mechanics, Chinese Academy of Sciences, Xi'an 710119, China; 2. University of Chinese Academy of Sciences, Beijing 100049, China; 3. Science and Technology on Low-Light-Level Night Vision Laboratory, Xi'an 710065, China)

Abstract: Since the concept of X-ray communication was introduced, there is a great deal of research on the core components, such as X-ray source, receiving antenna and X-ray detectors. However, few people focus on the theoretical basis. Therefore, this paper aims at establishing a primary theoretical model of X-ray communication. At start, the power transmission process that to establish the link power equation was analysed. In addition, bit error ratio model based on Poisson distribution was established by analysing major noise sources. After that, the core parameters of X-ray communication, such as transmitting speed, communication distance, bit error ratio can be decided by a giving transmission power. Finally, in order to verify the bit error ratio model and link power equation, the signal photons of micro channel plate detector output under various X-ray anode voltage and modulations was testified. Experimental results accorded well with the theoretical analysis, OOK and 4-PPM modulation model can achieve 10^{-4} to 10^{-5} bit error ratio level. These models would improved the transmission theory and laid foundations for the application of future spatial X-ray communication to some extent.

Key words: X-ray communication; bit error rate; Poisson noise model

CLC number: TN012 **Document code:** A **DOI:** 10.3788/IRLA201847.0622001

空间 X 射线通信系统误码率分析

李 瑶^{1,2}, 苏 桐^{*1,2}, 石 峰³, 盛立志¹, 强鹏飞^{1,2}, 赵宝升¹

(1. 中国科学院西安光学精密机械研究所 瞬态光学与光子技术重点实验室, 陕西 西安 710119; 2. 中国科学院大学, 北京 100049; 3. 微光夜视技术重点实验室, 陕西 西安 710065)

摘 要: 自 X 射线通信的概念被提出后, 大部分研究集中在发射源、收发天线和探测器等关键器件上, 而关于传输理论的研究较少。文中旨在建立 X 射线通信的理论模型, 首先建立了 X 射线通信的功率传输模型和链路方程; 其次建立了基于泊松噪声的 X 射线通信误码率模型, 随后建立了 X 射线通信中的核心参数: 通信距离, 通信速率, 误码率与传输功率之间的关系; 最后对不同阳极高压与不同调制方式下探测器端信号光子数进行实验监测, 对功率传输方程及误差模型进行验证, 测试了 X 射线通信系统的误码率, 理论与实验较为符合, OOK 和 4 PPM 的误码率可达 10^{-4} ~ 10^{-5} 量级, 为空间 X 射线通信研究建立了理论基础, 同时有望对空间 X 射线通信的工程化提供一定的参考。

关键词: X 射线通信; 误码率; 泊松模型

收稿日期: 2018-01-05; 修订日期: 2018-02-15

基金项目: 国家自然科学基金(61471357)

作者简介: 李瑶(1989-), 男, 博士生, 主要从事 X 射线通信方面的研究。Email: liyao@opt.cn

导师简介: 赵宝升(1959-), 男, 研究员, 主要从事单光子探测方面的研究。Email: open@opt.ac.cn

通讯作者: 苏桐(1988-), 男, 助理研究员, 博士, 主要从事 X 射线探测器方面的研究。Email: sutong@opt.ac.cn

0 Introduction

X-rays is a form of electromagnetic radiation. Most X-rays have a wavelength ranging from 0.01 to 10 nm. X-ray communication(XCOM) is a method which applying X-ray as carriers to transmit information in space^[1]. Compared with other space communication methods, XCOM has following merits. Firstly, because of the high frequency characteristic, XCOM offers larger available band, higher system bandwidth, as well as the strong anti-interference ability. Secondly, considering the small divergence angle of X-ray source and X-ray focusing optics, secure communication and high speed data transmission become possible^[2-3]. Specifically, Porter George thinks that the maximum theoretical rate of XCOM can reach 40 000 Tbps^[4].

The National Aeronautics and Space Administration (NASA) first introduced the concept of XCOM in 2007 and regarded it as a "revolutionary concept". In NASA's method, an UV LED is set to generate modulated electrons, then electrons are multiplied and accelerated to bombard the anode target to generate X-ray. In terms of the receiving side, the modulated X-ray will be captured by a PIN detector. In 2016, NASA proposed their new technology, called 'NavCube', a computing platform, which will be used to modulate X-ray source and demonstration XCOM in space in 2018^[3].

At the meantime, Catherine Kealhofer from Stanford University proposed a different emitting method which applying a femtosecond laser to modify the field emission to generate modulated X-ray^[5]. This method has advantages of small size and fast modulation but a limited X-ray photons.

In 2012, Zhao proposed a space XCOM scheme based on a grid-control X-ray tube and the MCP detector^[6]. As the modulation part, Grid-control X-ray tube can cut off electrons flow and this method increases the X-ray transferring efficiency^[7] dramatically.

Researchers have developed a number of studies on key devices such as transmitting devices and detectors since the concept was introduced^[8-10]. However, there is little research on the transmission theory of XCOM. Therefore, factors that affecting core parameters, such as communication distance, communication rate and the bit error ratio(BER) are still uncertain^[11-13]. Therefore, it is necessary to investigate more details about transmission theory in order to have a good understanding of XCOM.

1 XCOM system analysis

1.1 Power transmission process of XCOM

Similar to other wireless communication systems, the XCOM system is consists of the transmitting device, antennas and the receiving device. The schematic of space X-ray Communication is depicted in Fig.1.

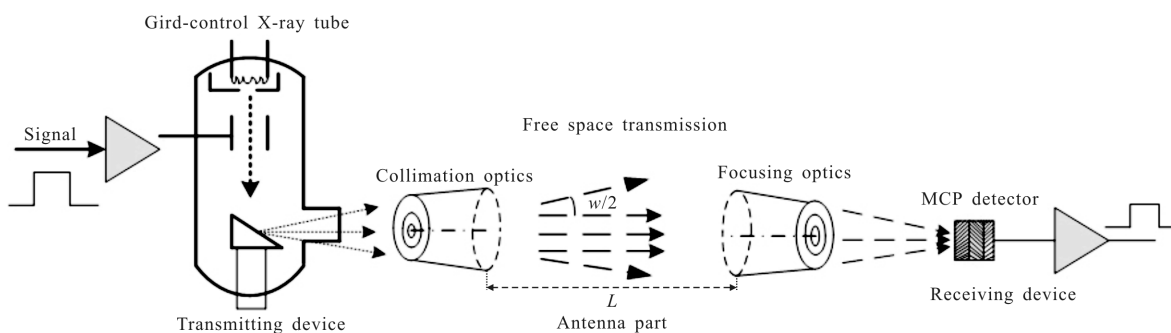


Fig.1 Schematic of space X-ray communication system

In the transmitting part, Grid-control X-ray tube can switch on and switch off electrons flow to load digital signal 1 or 0 into X-ray carriers, then the X-ray photons pass through antenna (collimation optics and focusing optics), received by the detector. Specifically, the power transmission process can be show as follows:

The emit power of X-ray source P_T is decided by electron power of X-ray source P_E and electron-photon conversion efficiency η , that is $P_T = P_E \cdot \eta$.

The effect of antenna is to minimum the divergence angle of emitted X-rays, it can be represented by the collimation gain G_C .

In the long distance space transmitting between collimation optical and focusing optical, signal X-ray power experienced the free space attenuation, which is inversely to the distance square. L is transmitting distance, $\omega/2$ is divergence angle after collimation, then the power per unit area P_A at the focusing optics part can be represented as:

$$P_A = \frac{P_T G_C}{\pi \left(L \tan \frac{\omega}{2} \right)^2} \quad (1)$$

The role of focusing optics is to increase the number of X-ray photons in the receive part. It can be measured by the effective collection area A_E .

The detector converts X-ray photons into electrical signal, it can be represented by the detector efficiency η_d . The detected X-ray power P_D can be expressed as:

$$P_D = \frac{P_T G_C A_E \eta_d}{\pi \left(L \tan \frac{\omega}{2} \right)^2} \quad (2)$$

where P_D is another form of communication speed, in other words, communication speed was restricted by the detected X-ray power P_D , then the relationship between transmitting distance and speed can be established.

1.2 XCOM system BER analysis

The BER of XCOM system can be expressed as the probability of errors in each single bit^[17]. BER of OOK modulation comes from the misjudgment of received photons, as each one photon appears at a

certain probability, the BER formula can be listed as follow:

$$PE = \frac{1}{2} \langle PE|1 \rangle + \frac{1}{2} \langle PE|0 \rangle \quad (3)$$

For a photon counting detector, the received photons according to the Poisson distribution in which $\langle PE|1 \rangle$ and $\langle PE|0 \rangle$ can be expressed as:

$$\langle PE|1 \rangle = \sum_{k=0}^{k_s} \frac{(k_s + k_n)^k}{k!} e^{-(k_s + k_n)} \quad (4)$$

$$\langle PE|0 \rangle = \sum_{k=k_t}^{+\infty} \frac{(k_n)^k}{k!} e^{-k_n} \quad (5)$$

In a IM/DD (Intensity modulation/direct detection) system, k_s represents the number of received signal photons per bit, k_n represents the average noise photons per bit, k_t is the threshold. When $k_s \geq k_t$, the receiver outputs logic 1. If $k_s < k_t$, the demodulation part exports logic 0. $\langle PE|1 \rangle$ and $\langle PE|0 \rangle$ represents the probability of misjudgment.

As a result, BER of XCOM system can be described as:

$$PE = \frac{1}{2} \langle PE|1 \rangle + \frac{1}{2} \langle PE|0 \rangle = \frac{1}{2} \left[\sum_{k=0}^{k_t} \frac{(k_s + k_n)^k}{k!} e^{-(k_s + k_n)} + \sum_{k=k_t}^{+\infty} \frac{(k_n)^k}{k!} e^{-k_n} \right] \quad (6)$$

This formula indicates that BER was determined by k_s , k_n and k_t . However, in experiments we cannot distinguish the MCP output whether resulting from X-ray photons or MCP noise. Namely, we cannot acknowledge the exact value of k_s and k_n . So we provide a new method to calculate k_n by transfer the dark current at MCP output side into equivalent X-ray photons at MCP input side. The electrons multiple process in a MCP detector was shown in Fig.2.

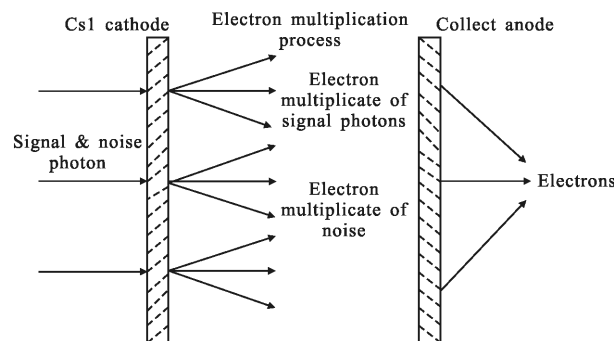


Fig.2 Electrons multiple process in the MCP detector

2 BER theoretical analysis

2.1 MCP detector noise analysis

The noise of MCP detectors are mainly comes from photocathode dark current and thermal noise^[18-19]. Photocathode dark current can be determined by formula (7):

$$i_d = aAT \exp\left[-\frac{W}{kT}\right] \quad (7)$$

where a is a coefficient decided by cathode material, A is the area of photocathode, T is material temperature in Kelvin, W is work function of the material and k is Boltzmann constant respectively.

The thermal noise of MCP detectors can be determined by formula (8):

$$\overline{i_{nL}^2} = \frac{4kT\Delta\nu}{R_L} \quad (8)$$

where R_L is equivalent load impedance, $\Delta\nu$ is bandwidth and T is temperature in Kelvin.

Since the multiplication in the channel is a random process, the MCP detectors will add additional noise to the multiplied signal, and factor F is introduced to describe the SNR change before and after multiplication^[20], it can be determined by formula (9) and (10).

$$\text{SNR}_{\text{out}} = \text{SNR}_{\text{in}} / \sqrt{F} \quad (9)$$

$$F = \frac{1}{\gamma} \cdot \left(1 + \frac{D^2}{K^2}\right) \quad (10)$$

where γ is the open air ration of the MCP detectors, D^2 is the variance of output electrons and \bar{K} is the average gain of MCP detectors.

In terms of our XCOM system, the equivalent cathode noise can be shown as:

$$i_n = aAT \exp\left[-\frac{W}{kT}\right] \cdot \sqrt{F} + \sqrt{\frac{4kT\Delta\nu}{R_L}} / \bar{K} \quad (11)$$

In this system, MCP was aligned in a Z shape and provide gain more than 10^6 level. The MCP detectors has a 50 mm diameter, $R_L = 50 \Omega$ equivalent load impedance, $\gamma = 0.7$ open air ration, 18.4 ns time resolution and 5.4×10^4 Hz bandwidth respectively. Usually, for a 120 nm thickness CsI photocathode, the

least energy required to produce a secondary electron is 7 eV^[21]. When $T = 300$ K, according to formula (11), in the MCP input part, the number of equivalent X-ray noise photons per second K_N can be calculated as formula(12):

$$K_N = \frac{1.78}{E \cdot \bar{K}} \times 10^{11} \text{ cps} \quad (12)$$

where E is the average energy of incident X-ray photons, which is related to the anode voltage, \bar{K} is the average gain of MCP detectors. From this formula, we have built the relationship between BER and MCP equivalent noise. Then we simulate the relationship between \bar{K} and K_N versus different incident X-ray energy E , which can be shown in Fig.3.

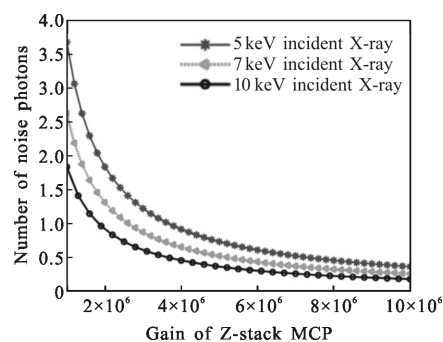


Fig.3 Relationship of \bar{K} and K_N against different incident X-ray energy

When use a Z-Stack MCP, \bar{K} is in 10^7 level^[21], E is 10 keV. The average number of noise photons per second should less than 2. Then we tested the average dark count rate of the Z-Stack MCP against different anode voltage. The MCP detector is Hamamatsu F1217 type, a GYU-6T high voltage power was used to supply the voltage of Z-Stack MCP detectors, each voltage is -300, -1 100 and -2 400 V respectively. Then a 10 minute dark count rate was counted under 1.3×10^{-4} Pa by three steps, regulate voltage, count the dark count rates and turn off the testing system. In order to achieve the dark count rate under 5, 7 and 10 keV X-ray photons, the anode voltage should be double, that is 10, 14 and 20 kV respectively. Experiment results can be shown in Tab.1,

theoretical analysis accords to the experiment results at a certain extent.

Tab.1 Z-Stack MCP dark count rate versus different anode voltages

Anode voltage/kV	Theoretical dark count rate/cps	Experiment results /cps
10	4-3	5-3
14	3-2	4-2
20	2.5-1.5	3-1

2.2 BER simulation of XCOM system

Normally, dark count rate is used to evaluate a MCP detector, MCP detectors perform a low dark count rate compared with other detectors, typical value should be 0.5-2 cps [22]. For instance, when transmitting signal in several kbps, for example 5 kbps, the dark count ratio k_n is about $4 \times 10^{-4} - 1 \times 10^{-4}$ counts per bit, far less than the received signal photons k_s per bit, so formula (6) can be expressed as follows:

$$PE = \langle PE|1 \rangle = \sum_{k=0}^{k_i} \frac{(k_s + k_n)^k}{k!} e^{-(k_s + k_n)} \approx \sum_{k=0}^{k_i} \frac{k_s^k}{k!} e^{-k_s} \quad (13)$$

Then we can calculate the required X-ray photons k_s against a changeable threshold k_i , which can be show in Tab.2.

Tab.2 Number of required k_s versus different k_i (OOK)

k_i	10^{-2} level	10^{-3} level	10^{-4} level	10^{-5} level	10^{-6} level
1	7	10	12	14	16
2	9	12	14	17	20
3	11	14	16	19	22
4	12	15	18	21	24
5	14	17	20	23	26

Similarly, BER level in the form of L-PPM modulation can be shown as formula (14):

$$PE = \langle PE|1 \rangle = \frac{1}{L} \sum_{k=0}^{k_i} \frac{(k_s + k_n)^k}{k!} e^{-(k_s + k_n)} \approx \frac{1}{L} \sum_{k=0}^{k_i} \frac{k_s^k}{k!} e^{-k_s} \quad (14)$$

where L is the carry digit, $L = 2^n$ (n is any positive integer), which represents the number of bits

(Minimum transmission unit) contained in a baud (Basic transmission unit). Usually, a L -PPM modulation has an average emission power of P/L , in which P is the optical power when transmitting a symbol 1.

Using 4 PPM modulation, $L = 4$, then the relationships between different BER level and k_s can be shown in Tab.3.

Tab.3 Number of required k_s versus different k_i (4 PPM)

k_i	10^{-2} level	10^{-3} level	10^{-4} level	10^{-5} level	10^{-6} level
1	3	6	8	11	13
2	4	7	10	13	15
3	5	9	12	15	18
4	6	10	13	17	19
5	7	11	15	18	21

3 Experiment

The schematic of BER testing model can be shown as Fig.4. Firstly, the input signal was modulated by OOK, 4 PPM individually, then the grid-control X-ray tube sent X-ray photons as streams. After that the X-ray photons were collimated and focused by Nested X-ray focusing optics (NXFO), then detected by a MCP detector placed on the remote focus. Finally, digital signal processing demodulated the MCP output and rebuilt the logic signal. This logic signal was connected to the FPGA-based BER counting module with a reference signal (initial output), and the BER counting module provided error numbers at per period.

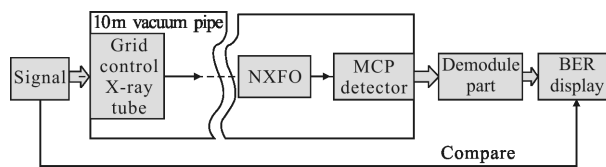


Fig.4 Schematic of BER testing

The BER testing experiment condition is 15 kV

anode voltage, 2.4 A filament current and -148 mV threshold voltage ($k_t = 1$) with OOK modulation, theoretical BER can be calculated by formula (13). When $k_t = 1$, theoretical and experimental BER results can be shown in Tab.4.

Tab.4 Theoretical and experimental BER against OOK modulation

V/kbps	BER number	Experimental BER level	Signal photons per bit (k_s)	Theoretical BER level
1.56	18/65 536	2.70×10^{-4}	14	1.2×10^{-5}
3.125	16/65 536	2.44×10^{-4}	12	7.9×10^{-5}
6.25	34/65 536	5.18×10^{-4}	10	4.5×10^{-4}
12.5	103/65 536	1.57×10^{-3}	9	1.2×10^{-3}
25	365/65 536	5.50×10^{-3}	8	3.0×10^{-3}

With 4 PPM modulation, theoretical BER can be calculated by formula (14). When $k_t = 1$, theoretical and experimental BER results can be shown in Tab.5.

Tab.5 Theoretical and experimental measured BER against 4 PPM modulation

V/kbps	BER number	Experimental BER level	Signal photons per bit (k_s)	Theoretical BER level
1.56	17/65 536	6.48×10^{-5}	13	7.9×10^{-6}
3.125	12/65 536	4.57×10^{-5}	12	2.0×10^{-5}
6.25	27/65 536	1.03×10^{-4}	10	1.2×10^{-4}
12.5	148/65 536	5.64×10^{-4}	8	2.8×10^{-4}
25	421/65 536	1.60×10^{-3}	7	7.5×10^{-4}

Our experimental results demonstrated that the BER level of XCOM system accorded well with theoretical calculation, PPM modulation has a less BER level than OOK modulation. In low speed communication situations ($V < 6.25$ kbps), BER of XCOM system can get $10^{-4} - 10^{-5}$ level. When the communication rate was about 25 kbps, BER of OOK and PPM modulation was about 10^{-3} level because the limited transmission power.

4 Conclusion

In this paper, we establish a theory that contains

two models. Model 1 gives the relationship between transmission rate and distance. Model 2 gives the relationship between transmitting X-ray power and BER. Experimental results show that to achieve 10^{-6} BER level, we need at least 13 photons; to achieve the rate of 100 kbps communication and 10 km transmitting distance, we need 27 mW transmitting X-ray power. These models can be used to describe the performance of X-ray communication system, and the experiment results could provide foundations for optimizing core parameters of XCOM system in our future works.

References:

- [1] Keith Gendreau. Next-generation communication [EB/OL]. [2017-10-1] http://gsfctechnology.gsfc.nasa.gov/TechSheet/XRAY_Goddard_Final.pdf, 2007.
- [2] Gorenstein P, Cash W, Gehrels N, et al. The future of high angular resolution X-ray astronomy [C]//Proceedings of SPIE, 2008, 7011: 2271816.
- [3] Keith Gendreau. Dr.Keith Gendreau talk about NICEER and Modulate X-ray Source [EB/OL]. [2016-2-12]. <https://www.nasa.gov/feature/goddard/2016/nasa-s-navcube>, 2016.
- [4] Porter George. See Straight Through Data Center Bandwidth Limitations with X-rays [EB/OL]. [2013-10-1]. http://cseweb.ucsd.edu/~gmporter/papers/porter_xray_tinytocs13.pdf, 2013.
- [5] Kealhofer C, Foreman S M, Gerlich S, et al. Ultrafast laser-triggered emission from hafnium carbide tips [J]. *Physical Review B*, 2011, 86(3): 165-173.
- [6] Sheng Lizhi, Zhao Baosheng, Zhou Feng, et al. Performance of the detection system for X-ray pulsar based navigation [J]. *Acta Photonica Sinica*, 2013, 42(9): 1071-1076. (in Chinese)
- [7] Zschornack. Handbook of X-Ray Data[M]. Berlin: Springer, 2007.
- [8] Ziegler E, Hignette O, Morawe C, et al. High-efficiency tunable X-ray focusing optics using mirrors and laterally-graded multilayers [J]. *Nuclear Instruments & Methods in Physics Research*, 2001, 467(2002): 954-957.
- [9] Jansson T, Gertsenshteyn M, Grubsky V, et al. Through-the-wall sensor systems based on hard X-ray imaging optics [C]//Proceedings of SPIE, 2007, 6538: A1-A9.

- [10] Song S, Xu L, Zhang H, et al. Novel X-ray communication based XNAV augmentation method using X-ray detectors[J]. *Sensors*, 2015, 15(9): 22325–22342.
- [11] Huang Long, Feng Guoying, Liao Yu. Free space optical communication based on supercontinuum laser source [J]. *Infrared & Laser Engineering*, 2015, 44(12): 3530–3534. (in Chinese)
- [12] Labiche J C, Mathon O, Pascarelli S, et al. Invited article: The fast readout low noise camera as a versatile X-ray detector for time resolved dispersive extended X-ray absorption fine structure and diffraction studies of dynamic problems in materials science, chemistry, and catalysis [J]. *Review of Scientific Instruments*, 2007, 78(9): 091301.
- [13] Wang Z, Wang X, Mu B. Nanoscale patterns made by using a 13.5-nm Schwarzschild objective and a laser produced plasma source[C]//Proceedings of SPIE, 2012, 8430(11): 34–38.
- [14] Tan A L, Yang Y, Ma J, et al. Influence of misalignment and aberrations on antenna received power in free-space laser communications[J]. *Optical Engineering*, 2009, 48(8): 73–80.
- [15] Ma J, Jiang Y, Yu S, et al. Packet error rate analysis of OOK, DPIM and PPM modulation schemes for ground-to-satellite optical communications [J]. *Optics Communications*, 2010, 283(2): 237–242.
- [16] Song S B, Xu L P, Zhang H, et al. X-ray communication based simultaneous communication and ranging [J]. *Chinese Physics B*, 2015, 24(9): 289–298.
- [17] Wang L Q, Su T, Zhao B S, et al. Bit error rate analysis of X-ray communication system [J]. *Acta Physica Sinica*, 2015, 64(12): 119–123. (in Chinese)
- [18] Chen B, Zhao B, Hu H, et al. X-ray photon-counting detector based on a micro-channel plate for pulsar navigation [J]. *Chinese Optics Letters*, 2011, 9(6): 13–16.
- [19] Henke B L, Knauer J P, Premaratne K. The characterization of X-ray photocathodes in the 0.1–10-keV photon energy region[J]. *Journal of Applied Physics*, 1981, 52(3): 1509–1520.
- [20] Shchemelev V N, Savinov E P. Total quantum-current yield in the soft X-ray region [J]. *Physics of the Solid State*, 1998, 40(6): 952–955.
- [21] Boutboul T, Akkerman A, Gibrekhterman A, et al. An improved model for ultraviolet-and x-ray-induced electron emission from CsI[J]. *Journal of Applied Physics*, 1999, 86(10): 5841–5849.
- [22] Hu Huijun, Zhao Baosheng, Sheng Lizhi, et al. X-ray photon counting detector for X-ray pulsar-based navigation [J]. *Acta Physica Sinica*, 2012, 61(1): 019701. (in Chinese)